Grain-size effect on ferroelectric $Pb(Zr_{1-x}Ti_x)O_3$ solid solutions induced by surface bond contraction

Haitao Huang*
Advanced Materials Research Center, School of Materials Engineering, Nanyang Technological University, Nanyang Avenue, Singapore 639798

Chang Q. Sun
School of Electrical Electronic Engineering, Nanyang Technological University, Nanyang Avenue, Singapore 639798

Zhang Tianshu and Peter Hing
Advanced Materials Research Center, School of Materials Engineering, Nanyang Technological University, Nanyang Avenue, Singapore 639798

(Received 6 July 2000; revised manuscript received 2 October 2000; published 23 April 2001)

Bond contraction in the surface layers induces a compressive stress on the inner part of a grain and results in a size effect for ferroelectric materials in the nanometer size range. By using the Landau-Ginsburg-Devonshire free energy approach, the phase transitions and intrinsic ferroelectric properties of the lead zirconate titanate solid solution system have been studied theoretically. It is found that, due to the surface bond contraction, the phase stability is affected by grain size and the size-dependent properties show differences in different phases.

DOI: 10.1103/PhysRevB.63.184112 PACS number(s): 77.80.−e, 77.70.+a, 77.22.−d, 05.70.−a

I. INTRODUCTION

The lead zirconate titanate solid-solution $Pb(Zr_{1-x}Ti_x)O_3$[PZT100$(1-x)$/100x] system has a lot of applications, such as in the smart structures[1] and memory devices.[2] As the ferroelectric device elements become smaller and smaller with the dimension of a ferroelectric in the submicrometer range or even lower, the properties become size dependent and the grain size effect should be taken into consideration in order to optimize the properties. The grain size dependence of the dielectric permittivity in barium titanate ceramics[3,4] and thin films[5] is known for many years. The Curie temperature, polarization, coercive field, switching speed, etc., all depend on the film thickness and grain size.[2] Several models have been proposed by different authors, which take into account effects such as the internal stresses,[3] the domain-wall contribution to the dielectric response,[4] and the shifts of the phase transition temperatures with grain size.[5] Theoretical approaches by using the transverse Ising model[6–10] and the Landau phenomenological theory[11–21] have also been tried. The latter has been more fruitful. The predicted critical size for ferroelectric such as $BaTiO_3$ was confirmed by experiments.[22,23] However, due to the complexity of the phenomenon, the origin of the grain size effect in fine-grained ferroelectric ceramics is still not well understood.

Recently, the effect of surface bond contraction is intensively studied. It is realized that the surface bond contraction plays an important role in the oxygen chemisorption,[24,25] the band-gap enlargement[26,27] of nanoclusters and the photoluminescence of nanometric SiO_2.[28] The surface bond contraction is expected to affect the materials properties when the materials are in nanometer range, i.e., when the surface-volume ratio becomes very large. In this paper, the gain size effect induced by the surface bond contraction is studied based on the Landau-Ginsburg-Devonshire (LGD) phenomenological theory. Useful results on intrinsic properties of nanosized PZT have been obtained. However, we have neglected the extrinsic contributions on properties, which are caused by domain wall, defect motion, and/or surface charge, etc. The extrinsic properties are more or less affected by the materials processing technology and discussion of them is out of the scope of the present study.

II. THEORY

According to Huang *et al.*,[29] for a curved surface the surface bond contraction induces a compressive stress σ_p on the inside grain

$$\sigma_p = -\frac{n^2 \delta a}{N^2 a} E, \tag{1}$$

where n is the number of unit cell layers which perform surface bond contraction ($n \leqslant 3$), N is the total number of unit cell layers along the radius direction of a spherical grain, a is the lattice constant, $\delta a/a$ is the ratio of surface bond contraction, and E is the Young's modulus. The negative sign is used here for compressive stress.

In order to study the effect of this compressive stress on the properties of ferroelectric PZT solid solution the LGD theory is used since, up to now, it is still one of the most powerful methods to study the effects of external fields on properties.[30–33] For ferroelectric PZT solid solution system, since the low-temperature rhombohedral phase has a tilting or rotation of the oxygen octahedra about the [111] axis, which does not occur in the high-temperature phase, the oxygen octahedral tilt angle together with the ferroelectric polarization are usually treated as order parameters.[34–43] For simplicity, the antiferroelectric polarization is omitted here since

we are more interested in ferroelectric phase. The elastic Gibbs free energy density function can be expressed as a Taylor series in powers of the order parameters and stress

$$\begin{aligned}\Delta G=&\alpha_1(P_1^2+P_2^2+P_3^2)+\alpha_{11}(P_1^4+P_2^4+P_3^4)+\alpha_{12}(P_1^2P_2^2+P_2^2P_3^2+P_3^2P_1^2)+\alpha_{111}(P_1^6+P_2^6+P_3^6)\\&+\alpha_{112}[P_1^4(P_2^2+P_3^2)+P_2^4(P_3^2+P_1^2)+P_3^4(P_1^2+P_2^2)]+\alpha_{123}P_1^2P_2^2P_3^2+\beta_1[\theta_1^2+\theta_2^2+\theta_3^2]+\beta_{11}[\theta_1^4+\theta_2^4+\theta_3^4]\\&+\gamma_{11}[P_1^2\theta_1^2+P_2^2\theta_2^2+P_3^2\theta_3^2]+\gamma_{12}[P_1^2(\theta_2^2+\theta_3^2)+P_2^2(\theta_3^2+\theta_1^2)+P_3^2(\theta_1^2+\theta_2^2)]\\&+\gamma_{44}[P_1P_2\theta_1\theta_2+P_2P_3\theta_2\theta_3+P_3P_1\theta_3\theta_1]-\frac{1}{2}s_{11}[X_1^2+X_2^2+X_3^2]-s_{12}[X_1X_2+X_2X_3+X_3X_1]\\&-\frac{1}{2}s_{44}[X_4^2+X_5^2+X_6^2]-Q_{11}[X_1P_1^2+X_2P_2^2+X_3P_3^2]-Q_{12}[X_1(P_2^2+P_3^2)+X_2(P_3^2+P_1^2)+X_3(P_1^2+P_2^2)]\\&-Q_{44}[X_4P_2P_3+X_5P_1P_3+X_6P_1P_2]-R_{11}[X_1\theta_1^2+X_2\theta_2^2+X_3\theta_3^2]-R_{12}[X_1(\theta_2^2+\theta_3^2)+X_2(\theta_3^2+\theta_1^2)+X_3(\theta_1^2+\theta_2^2)]\\&-R_{44}[X_4\theta_2\theta_3+X_5\theta_1\theta_3+X_6\theta_1\theta_2],\end{aligned}\tag{2}$$

where P_i $(i=1,2,3)$ is the magnitude of the ferroelectric polarization vector along the direction i; θ_i $(i=1,2,3)$ is the oxygen octahedral tilt angles; X_m $(m=1-6)$ is the stress; α_1, α_{ij} $(i,j=1,2)$ and α_{ijk} $(i,j,k=1,2,3)$ are the dielectric stiffness and higher-order dielectric stiffness coefficients at a constant stress; β_1 and β_{11} are the octahedral torsion coefficients; γ_{mn} $(m,n=1-6)$ is the coupling between the ferroelectric polarization and tilt angle; s_{ij} $(i,j=1-6)$ are the elastic compliance at constant polarization; Q_{ij} $(i,j=1-6)$ are the electrostrictive coupling between the ferroelectric polarization and stress; and R_{ij} $(i,j=1-6)$ are the rotostrictive coupling between the tilt angle and stress. The dielectric stiffness constant α_1 is assumed to be a linear function of temperature near the Curie point

$$\alpha_1=\frac{T-T_0}{2C\varepsilon_0},\tag{3}$$

where T is the temperature, T_0 is the Curie point, C is the Curie constant, and ε_0 is the vacuum dielectric permittivity. Amin *et al.* were among the first to determine the higher-order dielectric stiffness coefficients and calculate the dielectric, piezoelectric and elastic properties of the tetragonal, and high temperature rhombohedral phases at the morphotropic phase boundary (MPB) region.[44] Later, including the tilt of the oxygen octahedra in the LGD theory, the phase transition in the low temperature rhombohedral phase of $Pb(Zr_{0.8}Ti_{0.2})O_3$ was calculated.[45,46] With the steady accumulation of the experimental data, the coefficients in Eq. (2) for the entire PZT solid solution range can be obtained by fitting the theory with the experiment results. The best-fitted coefficients[34–38] are used in this paper. It has been assumed that all the coefficients in Eq. (2) except α_1 to be temperature independent.

It should be noted that when applying the LGD theory to a finite-size and inhomogeneous ferroelectrics, the total free energy instead of the energy density function is usually used,[19,47]

$$F=\int \lfloor g+D(\nabla P)^2\rfloor d\nu+\int D\lambda^{-1}P^2dS,\tag{4}$$

where the energy density g has the same form as Eq. (2), λ is the extrapolation length describing the difference between the surface and bulk, and D is connected with the correlation length. However, even for a very simple case, the spontaneous polarization and Curie temperature cannot be derived analytically from the above integration. In order to avoid the tedious numerical calculation and to find out the ''pure'' effect of the surface bond contraction, it is assumed that the surface and bulk have the same ferroelectric properties and the averaged value of polarization is used. The free energy density function of Eq. (2) will then be used instead of the total free energy.

The effect of the surface bond contraction can then be studied by substituting the following relation into Eq. (2):

$$X_1=X_2=X_3=\sigma_p,\quad X_4=X_5=X_6=0.\tag{5}$$

The Gibbs free energy is reduced to a simpler form

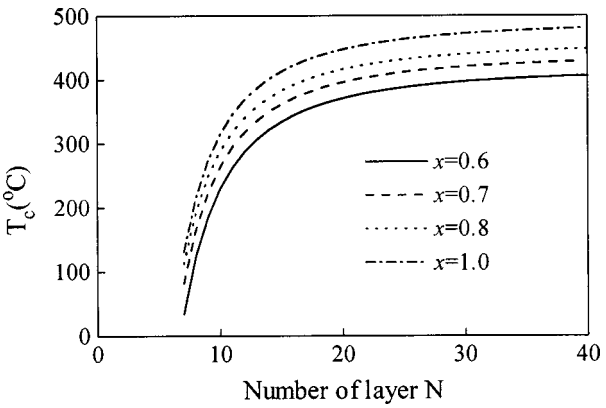

FIG. 1. Grain size dependent Curie temperature of tetragonal $Pb(Zr_{1-x}Ti_x)O_3$.

$$\Delta G=(\alpha_1-Q_h\sigma_p)(P_1^2+P_2^2+P_3^2)+\alpha_{11}(P_1^4+P_2^4+P_3^4)+\alpha_{12}(P_1^2P_2^2+P_2^2P_3^2+P_3^2P_1^2)+\alpha_{111}(P_1^6+P_2^6+P_3^6)$$
$$+\alpha_{112}[P_1^4(P_2^2+P_3^2)+P_2^4(P_3^2+P_1^2)+P_3^4(P_1^2+P_2^2)]+\alpha_{123}P_1^2P_2^2P_3^2+(\beta_1-R_h\sigma_p)[\theta_1^2+\theta_2^2+\theta_3^2]+\beta_{11}[\theta_1^4+\theta_2^4+\theta_3^4]$$
$$+\gamma_{11}[P_1^2\theta_1^2+P_2^2\theta_2^2+P_3^2\theta_3^2]+\gamma_{12}[P_1^2(\theta_2^2+\theta_3^2)+P_2^2(\theta_3^2+\theta_1^2)+P_3^2(\theta_1^2+\theta_2^2)]$$
$$+\gamma_{44}[P_1P_2\theta_1\theta_2+P_2P_3\theta_2\theta_3+P_3P_1\theta_3\theta_1]-\frac{3}{2}(s_{11}+2s_{12})\sigma_p^2, \quad (6)$$

where $Q_h=Q_{11}+2Q_{12}$ and $R_h=R_{11}+2R_{12}$.

The solutions which are of interest for ferroelectric PZT system are as follows.

(1) Paraelectric cubic phase P_C,

$$P_1=P_2=P_3=0, \quad \theta_1=\theta_2=\theta_3=0. \quad (7a)$$

(2) Ferroelectric tetragonal phase F_T,

$$P_1=P_2=0, \quad P_3^2\neq 0, \quad \theta_1=\theta_2=\theta_3=0. \quad (7b)$$

(3) Ferroelectric rhombohedral high-temperature phase $F_{R(HT)}$,

$$P_1^2=P_2^2=P_3^2\neq 0, \quad \theta_1=\theta_2=\theta_3=0. \quad (7c)$$

(4) Ferroelectric rhombohedral low-temperature phase $F_{R(LT)}$,

$$P_1^2=P_2^2=P_3^2\neq 0, \quad \theta_1^2=\theta_2^2=\theta_3^2\neq 0. \quad (7d)$$

The equilibrium values of the components of the order parameters can be determined by minimizing the free energy function of Eq. (6) with respect to the order parameters

$$\frac{\partial\Delta G}{\partial P_i}=\frac{\partial\Delta G}{\partial\theta_i}=0 \quad (i=1,2,3) \quad (8)$$

and at the same time satisfy the stability conditions. Various properties of the PZT in different phases can be obtained based on the equilibrium values of the order parameters.

III. RESULTS AND DISCUSSION

A. Curie temperature

The Curie temperature can be determined by equalizing the Gibbs free energy of the paraelectric and ferroelectric phases. Compared with the calculation of the bulk Curie temperature, it is easy to find out that the Curie temperature is shifted to lower temperature due to the surface bond contraction

$$T_C=T_{C\infty}+2C\varepsilon_0Q_h\sigma_p=T_{C\infty}-\frac{2n^2\delta a}{N^2a}C\varepsilon_0Q_hE, \quad (9)$$

where $T_{C\infty}$ is the Curie temperature of bulk materials with large grains.

Figure 1 shows the grain size dependence of the Curie temperature of the tetragonal PZT solid solution. According to Goldschmidt, ionic radius of an atom contracts with the reduction of the atomic coordination number, for example, it contracts by 4, 6, and 12 %, when the coordination number reduced from 12 to 8, 6, and 4, respectively.[48] Pauling has also noticed that the radius of a Cu atom contracts from 0.128 to 0.117 nm when its coordination number changes from 12 to 1.[49] For simplicity, it is assumed in this paper that the surface bond contracts by an average of 10% within the top three layers. The Young's modulus is chosen to be 200 GPa. This value is reasonable for tetragonal PZT as compared with the bulk modulus of 209 GPa for $PbTiO_3$ obtained by first-principles calculation.[50] It can be seen that the Curie temperature drops slowly with the number of unit cell layers N for $N>15$. For $N<15$, the Curie temperature drops dramatically. The equivalent grain size for $N=15$ is about 12 nm since the lattice parameter is about 0.4 nm as determined by Glazer *et al.*[51] A similar result for $PbTiO_3$ is confirmed in experiment.[52]

It should be pointed out that below certain grain size (critical size) the Curie temperature reaches 0 K which implies a lost of ferroelectricity. This critical size obtained by the present model is about 4 nm ($N=5$). This value is comparable with the theoretical value of 4.2 nm obtained by Zhong *et al.*[19] They have used the total free energy of Eq. (4) to study the size effect in $PbTiO_3$. However, this critical size is smaller than those obtained by various experiments, such as 12.6 nm by Raman scattering,[53] 8.8 nm by specific heat measurement,[54] 7 nm by x-ray diffraction.[52] This could be due to the oversimplification of our model but a more sensitive measurement is needed to verify different theoretical models since the existing results are too scattering.

The effect of surface bond contraction on the Curie temperature for the entire composition range of the ferroelectric PZT solid solution is depicted in Fig. 2. Here the composition is restricted to the ferroelectric PZT with a mole fraction of $PbTiO_3$ higher than 0.1 since the bulk Curie temperature can only be well fitted within this composition range. It can be seen from Fig. 2 that the Curie temperature decreases with decreasing grain size (i.e., decreasing N) in the entire composition range. However, this decrease is not uniform. At a composition range near the MPB, i.e., $x=0.5$, the Curie temperature is less affected by the grain size. This is due to the composition dependence of the Curie constant and the electrostrictive constant Q_h.

The Curie constant and the electrostrictive constant are both composition dependent. The Curie constant varies with increasing amount of $PbTiO_3$ from around 2×10^5 °C at the pure $PbZrO_3$ side to about 1.5×10^5 °C at the pure $PbTiO_3$ side with a maximum of about 4.25×10^5 °C at the MPB.

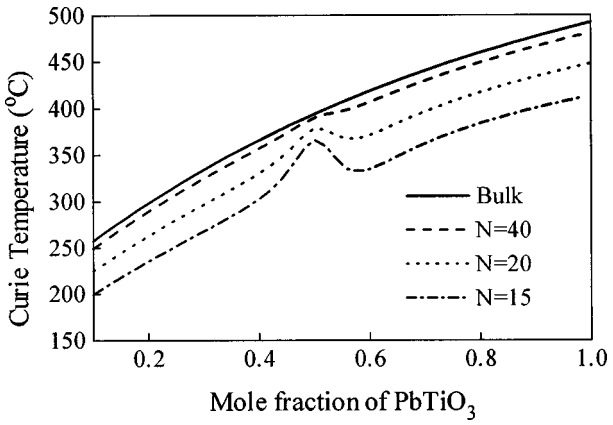

FIG. 2. Grain size effect on the Curie temperature for $Pb(Zr_{1-x}Ti_x)O_3(x \geqslant 0.1)$. (In this figure and hereafter, ''bulk'' is used to indicate very big grains.)

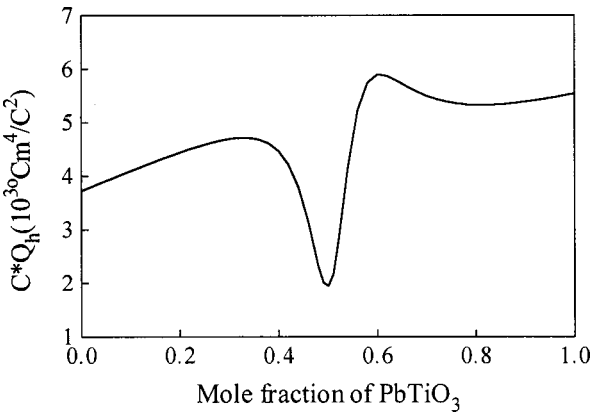

FIG. 3. Composition dependence of the C^*Q_h value.

However, the electrostrictive constant shows a slight increase with increasing amount of $PbTiO_3$ except a minimum is found also at the MPB. As shown in Fig. 3, the multiplication of the Curie constant by the electrostrictive constant is found to have a minimum at the MPB and a maximum near the MPB with about 0.6 mole fraction of $PbTiO_3$. This behavior of the multiplication explains the size dependence effect of the Curie temperature shown in Fig. 2. According to Eq. (9), the PZT 50/50 is nonsensitive to the grain size effect since the multiplication C^*Q_h is a minimum at this composition. While the tetragonal PZT 40/60 is most effectively affected by the grain size since the multiplication C^*Q_h is a maximum at this composition. It can also be concluded that the electrostrictive constant Q_h is the dominant factor in the multiplication value of C^*Q_h since this value is minimum at the MPB although the Curie constant C shows a maximum at this composition. An implication of this finding is that, in the materials engineering, it is possible to modify the size dependence behavior of the Curie temperature by adjusting the Q_h value, i.e., the ratio of Q_{11}/Q_{12}. It is obvious that when the ratio of Q_{11}/Q_{12} becomes -2, the Q_h is zero, and the Curie temperature is independent of the size at all.

B. Spontaneous polarization

The spontaneous polarization can be obtained by minimizing the Gibbs free energy and at the same time satisfying the stability of the ferroelectric state

$$F_T:\ P_3^2=\frac{-\alpha_{11}+[\alpha_{11}^2-3\alpha_{111}(\alpha_1-Q_h\sigma_p)]^{1/2}}{3\alpha_{111}}, \tag{10a}$$

$$F_{R(HT)}:\ P_3^2=\frac{-(\alpha_{11}+\alpha_{12})+\sqrt{(\alpha_{11}+\alpha_{12})^2-(\alpha_1-Q_h\sigma_p)(3\alpha_{111}+6\alpha_{112}+\alpha_{123})}}{3\alpha_{111}+6\alpha_{112}+\alpha_{123}}, \tag{10b}$$

$$F_{R(LT)}:\ P_3^2=\frac{-b+\sqrt{b^2-4\xi c}}{2\xi}, \tag{10c}$$

$$\theta_3^2=-\frac{\beta_1-R_h\sigma_p+\phi P_3^2}{2\beta_{11}}, \tag{10d}$$

where

$$\xi=3\alpha_{111}+6\alpha_{112}+\alpha_{123},\quad \phi=\gamma_{11}+2\gamma_{12}+\gamma_{44},$$

$$b=\frac{2}{3}\zeta-\frac{\phi^2}{2\beta_{11}},\quad \zeta=3(\alpha_{11}+\alpha_{12}),$$

$$c=\alpha_1-Q_h\sigma_p-\frac{\beta_1-R_h\sigma_p}{2\beta_{11}}\phi.$$

For the tetragonal phase the spontaneous polarization P_S is equal to P_3, while for the rhombohedral phase, P_S is equal to $\sqrt{3}P_3$.

The room temperature spontaneous polarization of tetragonal PZT is shown in Fig. 4. It decreases with decreasing grain size. Similar to the Curie temperature, the spontaneous polarization decreases slowly with N for $N>15$. When $N<15$, it drops fast. Similar trend for $PbTiO_3$ is experimentally verified by Chattopadhyay *et al.*[52] as they found that the lattice parameter c decreases and a increases when the grain

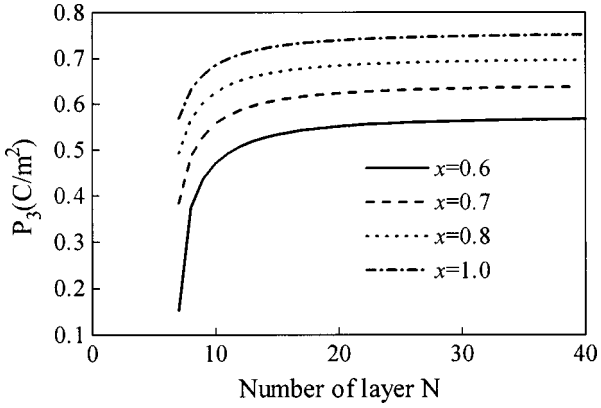

FIG. 4. Room temperature spontaneous polarization of tetragonal $Pb(Zr_{1-x}Ti_x)O_3$ ($x=0.6$, 0.7, 0.8, and 1.0).

size decreases below 100 nm. The resulting reduction in the tetragonal distortion (c/a) implies a decrease in spontaneous polarization. The room temperature spontaneous polarization becomes zero for grain size below 5.6 nm ($N=7$). This is an indication of room temperature phase transition from the ferroelectric to paraelectric at this grain size. As the temperature increases, the grain size at which this phase transition takes place also increases.

The temperature dependence of the spontaneous polarization of the tetragonal PZT ceramics under different grain size is shown in Fig. 5. In general, the spontaneous polarization decreases with increasing temperature. When the grain size decreases, the spontaneous polarization is depressed. This depression is more significant at higher temperatures. A decrease in the Curie temperature can thus be expected due to the reduction in the spontaneous polarization. For PZT 30/70, the spontaneous polarization vanishes at the Curie temperature showing a second-order phase transformation from the ferroelectric phase to the paraelectric one. However, the spontaneous polarization of PZT 20/80 does not go to zero when approaching the Curie temperature from the ferroelectric side due to its first-order nature of the $F_T \rightarrow P_C$ phase transformation.

For rhombohedral PZT, in order to calculate the spontaneous polarization the rotostrictive coefficient R_h which is

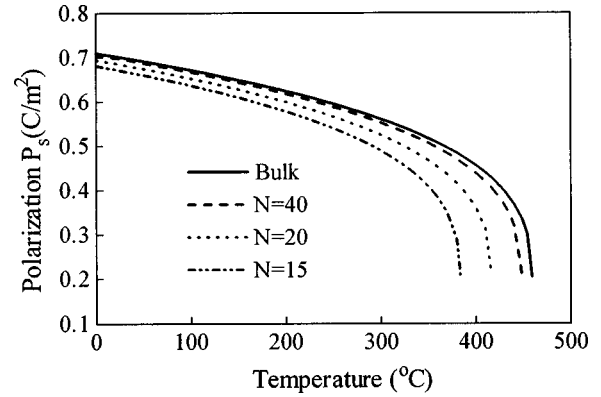

FIG. 5. Temperature dependence of the spontaneous polarization of PZT 20/80 with different grain sizes.

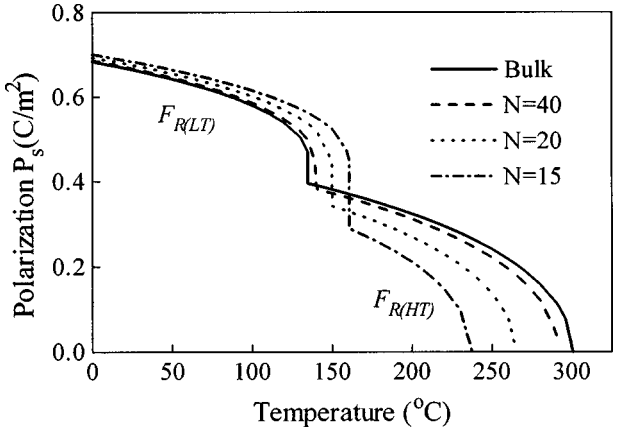

FIG. 6. Temperature dependence of the spontaneous polarization of PZT 80/20 with different grain sizes.

related to the coupling of oxygen octahedron and the stress should be known. However, due to the lack of experimental data, this value is not determined yet. Oh *et al.*[41–43] have estimated this value by extrapolating the lattice constants obtained by Glazer *et al.*[51] into the low temperature rhombohedral phase. The rotostrictive coefficient thus obtained for PZT 90/10 is slightly temperature dependent. For simplicity we assume the value to be independent of temperature and composition, just as other investigators have done in the case of R_{44}.[36–40] The averaged value of the rotostrictive coefficient, $-1.553\times10^{-4}\,\mathrm{deg}^{-2}$, is chosen in the present calculation.

The temperature dependence of the spontaneous polarization of the rhombohedral PZT 80/20 is shown in Fig. 6. For PZT 80/20 with very big grains, the spontaneous polarization shows a kink at the $F_{R(LT)} \rightarrow F_{R(HT)}$ phase transition temperature T_R, which means that the $F_{R(LT)} \rightarrow F_{R(HT)}$ phase transition is first order. With decreasing grain size, the spontaneous polarization of the $F_{R(HT)}$ phase decreases, while, on the contrary, that of the $F_{R(LT)}$ phase increases. With decreasing grain size, the temperature range at which the $F_{R(HT)}$ phase is stable also decreases. For very big grains, this temperature range of a stable $F_{R(HT)}$ phase is about 165 °C. It drops to about 70 °C when the grain size is about 12 nm ($N=15$). The $F_{R(LT)} \rightarrow F_{R(HT)}$ phase transition temperature is found to increase with decreasing grain size. The size-dependent phase transition temperature T_R can be derived as

$$T_R = T_{R\infty} + 2\varepsilon_0 C\left(Q_h - \frac{R_h \phi}{2\beta_{11}}\right)\sigma_p, \tag{11}$$

where $T_{R\infty}$ is the $F_{R(LT)} \rightarrow F_{R(HT)}$ phase transition temperature of bulk materials with very big grains. Its best fitted value for the PZT solid solution can be found in Refs. 36–40.

The size dependence of the $F_{R(LT)}$-$F_{R(HT)}$ phase transition temperature T_R is shown in Fig. 7. T_R increases slightly with decreasing grain size until it reaches the Curie temperature. At this grain size the $F_{R(HT)}$ phase is completely unstable and will not appear in the whole temperature range.

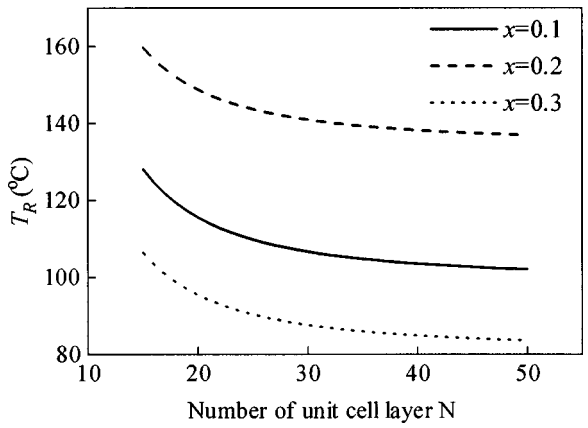

FIG. 7. Size dependence of T_R of rhombohedral $Pb(Zr_{1-x}Ti_x)O_3$ ($x=0.1$, 0.2, and 0.3).

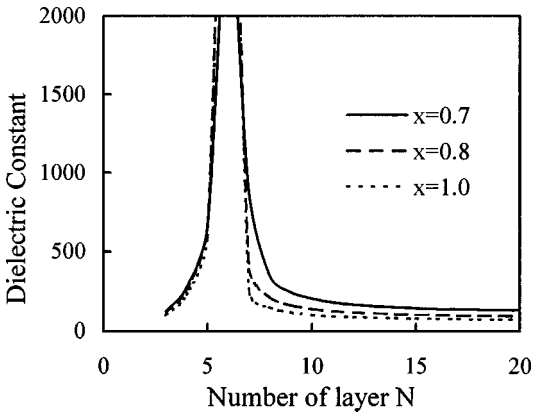

FIG. 9. Room temperature dielectric constant of $Pb(Zr_{1-x}Ti_x)O_3$ ($x=0.7$, 0.8, and 1.0) vs number of unit cell layers.

The unstableness of the $F_{R(HT)}$ phase can also be anticipated according to the Le Chatelier's principle. Since, as can be seen from the thermal expansion curve of PZT 92/8 shown in Fig. 8, the volume of the $F_{R(HT)}$ phase is larger than that of the P_C or the $F_{R(LT)}$ phase.[55] The surface bond contraction induced compressive stress favors the stableness of the phase with smaller volume and thus decreases the stability of the $F_{R(HT)}$ phase.

C. Dielectric constant

The dielectric constant can be determined from the reciprocal of the dielectric stiffness matrices ($\chi_{ij}=\varepsilon_0\partial^2\Delta G/\partial P_i\partial P_j$) by using the following relation:

$$\varepsilon_{ij}=A_{ij}/\Delta, \tag{12}$$

where A_{ij} and Δ are the cofactor and determinant of the χ_{ij} matrix.

The size dependence of the room temperature dielectric constant for tetragonal PZT is shown in Fig. 9. A dielectric anomaly can be clearly seen which indicates a phase transformation from a ferroelectric phase to a paraelectric one. The size at which this phase transition takes place is about 5.6 nm ($N=7$). It is the same size at which the spontaneous polarization becomes zero. The dielectric constant in the F_T phase increases while that in the P_C phase decreases with decreasing grain size. Similar result is obtained by using the total free energy of Eq. (4).[47] However, this result differs from the experimental work of Chattopadhyay *et al.*[52] They found the dielectric constant decreases with decreasing size in a size range of 26–100 nm. The reason is that our calculation has not taken the domain wall contribution into account so that the calculated relative permittivity is lower than the experimental value. Actually the domain wall contribution has an opposite effect as compared with the surface bond contraction induced effect. When the grain size decreases to a value comparable to the width of domain walls, pinning points would develop inside the grains and the domain wall motion would be inhibited.[52] The reduced wall mobility will cause a decrease in the relative permittivity. The measured value is a competition between the increase of relative permittivity by surface bond contraction and the decrease of the relative permittivity by domain wall pinning. From our model, in the size range of 26–100 nm ($60<N<240$), the increase in the dielectric constant due to the surface bond contraction is negligible. The domain wall pinning effect thus dominates in this size range and result in a decrease in the measured dielectric constant.

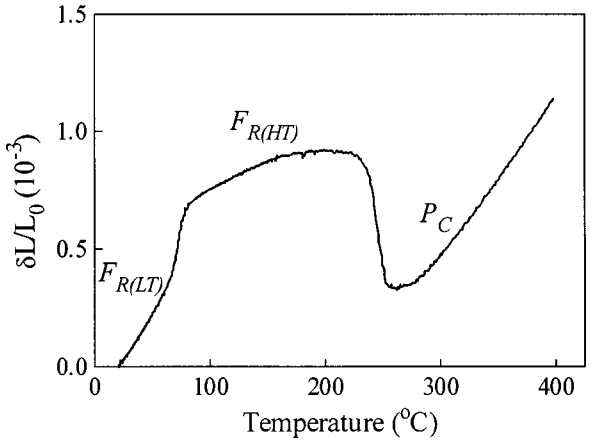

FIG. 8. Thermal expansion curve of PZT 92/8 showing three consecutive phase transitions: $F_{R(LT)}\rightarrow F_{R(HT)}\rightarrow P_C$.

The temperature dependence of the dielectric constant of PZT 30/70 is shown in Fig. 10. The dielectric constant goes to infinite when approaching the Curie temperature since the F_T to P_C phase transition for PZT 30/70 is second order. The Curie temperature also decreases with decreasing grain size. The dielectric constant shows an opposite trend of grain size dependence when across the phase transition temperature T_C. That is, in the F_T phase the dielectric constant increases with decreasing grain size while in the P_C phase it decreases. Similar behavior is found for PZT 20/80 except that the dielectric constant shows a sharp peak at the Curie temperature due to its first order kind of $F_T\rightarrow P_C$ phase transformation. The Curie temperature and the peak dielectric constant both decrease with decreasing grain size.

The temperature dependence of the dielectric constant of rhombohedral PZT 80/20 which has a continuous phase transformation $F_{R(LT)}\rightarrow F_{R(HT)}\rightarrow P_C$ with increasing temperature is shown in Fig. 11. The dielectric constant goes to

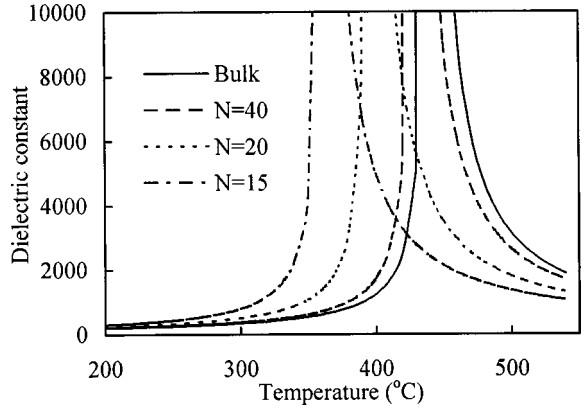

FIG. 10. Temperature dependence of the dielectric constant of PZT 30/70.

infinite at the Curie temperature due to the second order nature of the $F_{R(HT)} \rightarrow P_C$ phase transformation. The Curie temperature decreases with reducing grain size. Same as that of the tetragonal PZT, the paraelectric dielectric constant of PZT 80/20 decreases with the grain size but the rhombohedral high temperature dielectric constant increases with decreasing grain size.

The temperature dependence of the dielectric constant of PZT 80/20 near the $F_{R(LT)} \rightarrow F_{R(HT)}$ phase transformation is enlarged in Fig. 11(b). The sudden jump in dielectric constant at the phase transition temperature T_R is indicative of a first order transition. The magnitude of the dielectric jump increases with decreasing size which means the phase transition becomes more and more of the first order kind. As clearly seen from the figure the transition temperature T_R increases with the decreasing size. Once again the trend of size dependence of the dielectric constant is changed across the transition temperature T_R, i.e., the dielectric constant of the $F_{R(HT)}$ phase increases with the decreasing size while that of the $F_{R(LT)}$ phase decreases with size.

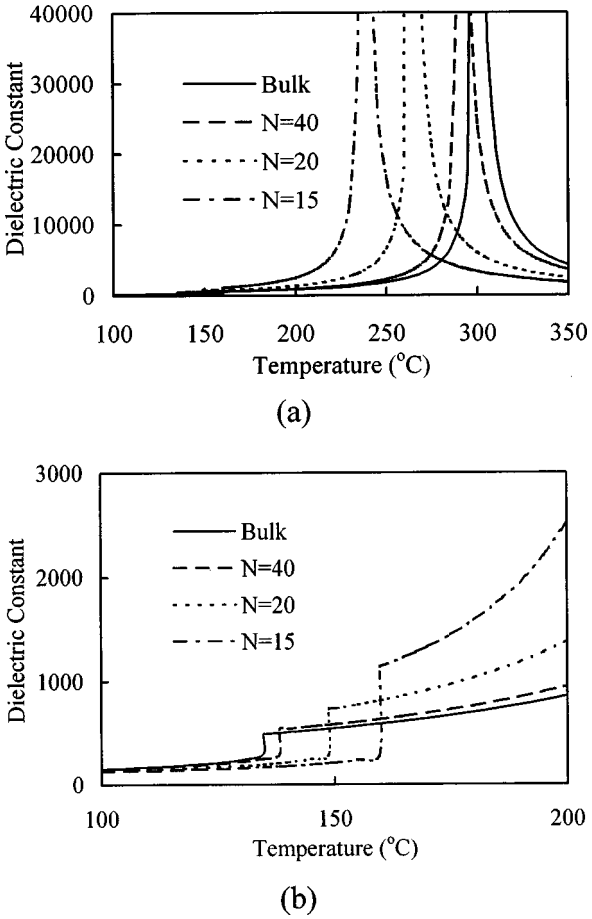

FIG. 11. Temperature dependence of the dielectric constant of PZT 80/20 in (a) 100–350 °C and (b) 100–200 °C.

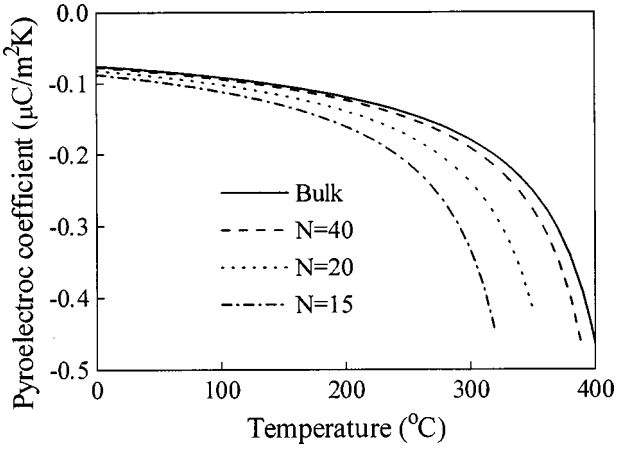

FIG. 12. Temperature dependence of the pyroelectric coefficient of PZT 30/70.

D. Pyroelectric properties

The pyroelectric coefficient can be calculated directly by differentiating the spontaneous polarization with temperature. As shown in Fig. 12, in general, the pyroelectric coefficient is negative since the spontaneous polarization decreases with temperature. The absolute value of the pyroelectric coefficient increases with temperature and goes to infinite when approaching the Curie temperature. For tetragonal PZT, the absolute value of pyroelectric coefficient is found to increase with decreasing grain size. It seems promising for the infrared detection application. However, in real application the figure of merit ($F_V = p/\varepsilon$, where p is the pyroelectric coefficient), which characterizes the voltage response[56] is more important than the pyroelectric coefficient itself. Higher F_V is always sought for. Unfortunately, it is found that this figure of merit decreases with decreasing size as shown in Fig. 13. Although the pyroelectric coefficient goes to infinite at the Curie temperature, the figure of merit F_V decreases with increasing temperature. This is due to the fact that the dielectric constant increases much faster with the temperature than the pyroelectric coefficient does. It can be derived that for the F_T phase, the pyroelectric coefficient p is

$$p = \frac{dP_3}{dT} = -\frac{1}{8\varepsilon_0 C P_3 \sqrt{\alpha_{11}^2 - 3\alpha_{111}(\alpha_1 - Q_h \sigma_p)}}. \quad (13)$$

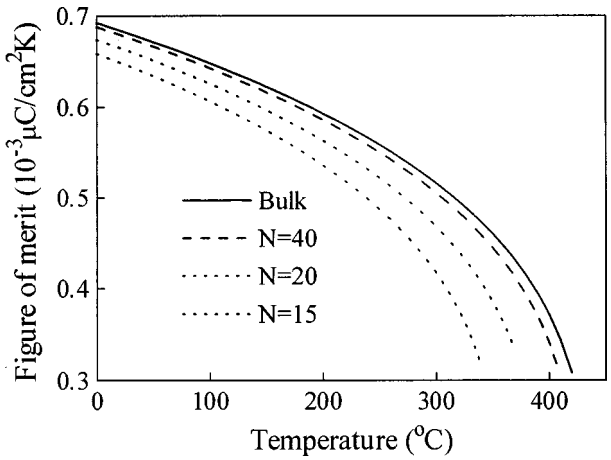

FIG. 13. Temperature dependence of the figure of merit F_V of PZT 30/70.

The figure of merit F_V is only a function of spontaneous polarization

$$F_V = p_T/\varepsilon_{33} = -\frac{P_3}{C}. \tag{14}$$

For PZT 30/70 with a second order phase transformation, both the figure of merit F_V and the spontaneous polarization go to zero at the Curie temperature.

E. Surface bond contraction ratio $\delta a/a$

The surface bond contraction ratio $\delta a/a$ assumed in this paper is 10%. This may be a little bit overestimated. Due to the lack of experiment data, the exact value is not known. From Eqs. (9) and (11), it can be seen that the phase transition temperatures T_C and T_R are both linear functions of the ratio $\delta a/a$ though they show different trends with this ratio. The Curie temperature T_C decreases while the $F_{R(LT)}$ to $F_{R(HT)}$ phase transition temperature T_R increases with increasing bond contraction ratio $\delta a/a$. The spontaneous polarization P_S, the dielectric constant ε, the pyroelectric coefficient p, and the figure of merit F_V have much more complicated relations with the ratio $\delta a/a$ than the phase transition temperatures do. Generally, the P_S, ε (of the P_C or the $F_{R(LT)}$ phase), and F_V all decrease with increasing ratio $\delta a/a$ while the ε (of the $F_{R(HT)}$ phase) and the absolute value of p both increase with the ratio $\delta a/a$.

IV. CONCLUSION

The surface bond contraction induces a compressive stress on the inner part of a grain and this effect should be taken into account for ferroelectric materials in the nanometer size range. The induced stress causes decreases of the Curie temperature and spontaneous polarization (except in the $F_{R(LT)}$ phase) with decreasing grain size. A size driven dielectric anomaly indicating a ferroelectric to paraelectric phase transition can be seen due to the surface bond contraction. The theoretical results correspond well with experiments done by other investigators. Our model predicts that the $F_{R(LT)} \rightarrow F_{R(HT)}$ phase transition temperature T_R increases with decreasing size and the $F_{R(HT)}$ phase is unstable for small size ferroelectrics. The dielectric constant shows opposite trend of dependence on the grain size across the transition temperatures T_C and T_R. The temperature dependence of the pyroelectric coefficient is similar to that of the spontaneous polarization. The figure of merit decreases with decreasing grain size. Linear relations exist between the phase transformation temperatures (T_C and T_R) and the surface bond contraction ratio $\delta a/a$. However, experimental information on the value of surface bond contraction ratio of ferroelectric materials is still needed for a more precise description of the effect induced by surface bond contraction.

*Author to whom correspondence should be addressed. Electronic address: hthuang@ntu.edu.sg

[1] R. E. Newnham, MRS Bull. **22**, 20 (1997).
[2] J. F. Scott and C. A. Paz de Araujo, Science **246**, 1400 (1989).
[3] W. R. Buessem, L. E. Cross, and A. K. Goswami, J. Am. Ceram. Soc. **49**, 33 (1966).
[4] G. Arlt and N. A. Pertsev, J. Appl. Phys. **70**, 2283 (1991).
[5] R. Waser, Integr. Ferroelectr. **15**, 39 (1997).
[6] M. G. Cottam, D. R. Tilley, and B. Zeks, J. Phys. C **17**, 1793 (1984).
[7] F. Aguilera-Granja and J. L. Moran-Lopez, Solid State Commun. **74**, 155 (1990).
[8] C. L. Wang, W. L. Zhong, and P. L. Zhang, J. Phys.: Condens. Matter **3**, 4743 (1992).
[9] H. K. Sy, J. Phys.: Condens. Matter **5**, 1213 (1993).
[10] W. L. Zhong, C. L. Wang, P. L. Zhang, and Y. G. Wang, Ferroelectrics **229**, 11 (1999).
[11] D. L. Mills, Phys. Rev. B **3**, 3887 (1971).
[12] I. P. Batra, P. Wurfel, and B. D. Silverman, Phys. Rev. B **7**, 3275 (1973).
[13] T. C. Lubensky and M. H. Rubin, Phys. Rev. B **12**, 3885 (1975).
[14] R. Krestschmer and K. Binder, Phys. Rev. B **20**, 1065 (1979).
[15] K. Binder, Ferroelectrics **35**, 99 (1981).
[16] D. R. Tilly and B. Zeks, Solid State Commun. **49**, 823 (1984).
[17] J. F. Scott, H. M. Duiker, P. D. Beale, B. Pouligny, K. Dimmler, M. Parris, D. Butler, and S. Eaton, Physica B **150**, 160 (1988).
[18] D. R. Tilly and B. Zeks, Ferroelectrics **134**, 313 (1992).
[19] W. L. Zhong, Y. G. Wang, P. L. Zhang, and B. D. Qu, Phys. Rev. B **50**, 698 (1994).
[20] Y. G. Wang, W. L. Zhong, and P. L. Zhang, Solid State Commun. **90**, 329 (1994).
[21] W. L. Zhong, B. D. Qu, P. L. Zhang, and Y. G. Wang, Phys. Rev. B **50**, 12 375 (1994).
[22] S. Schlag and H. F. Eicke, Solid State Commun. **91**, 883 (1994).
[23] S. Schlag, H. F. Eicke, and W. B. Stern, Ferroelectrics **173**, 351 (1995).
[24] C. Q. Sun and C. L. Bai, J. Phys. Chem. Solids **58**, 903 (1997).
[25] C. Q. Sun, Vacuum **48**, 535 (1997).
[26] C. Q. Sun, Appl. Phys. Lett. **72**, 1706 (1998).
[27] C. Q. Sun and P. Hing, Surf. Rev. Lett. **6**, L465 (1999).
[28] C. Q. Sun, X. W. Sun, H. Q. Gong, H. Huang, H. Ye, D. Jin, and P. Hing, J. Phys.: Condens. Matter **11**, L547 (1999).

[29] H. Huang, C. Q. Sun, and P. Hing, J. Phys.: Condens. Matter **12**, L127 (2000).
[30] L. D. Landau and E. M. Lifshitz, *Statistical Physics*, Vol. 5 of Course of Theoretical Physics (Pergamon Press, New York, 1980), Pt. I.
[31] D. Damjanovic, Rep. Prog. Phys. **61**, 1267 (1998).
[32] G. A. Smolenskii, *Ferroelectrics and Related Materials* (Gordon and Breach Science, New York, 1984).
[33] B. A. Strukov and A. P. Levanyuk, *Ferroelectric Phenomena in Crystals* (Springer-Verlag, Berlin, 1998).
[34] M. J. Haun, E. Furman, S. J. Jang, and L. E. Cross, Ferroelectrics **99**, 13 (1989).
[35] M. J. Haun, E. Furman, M. A. McKinstry, and L. E. Cross, Ferroelectrics **99**, 27 (1989).
[36] M. J. Haun, Z. Q. Zhuang, E. Furman, S. J. Jang, and L. E. Cross, Ferroelectrics **99**, 45 (1989).
[37] M. J. Haun, E. Furman, T. R. Halemane, and L. E. Cross, Ferroelectrics **99**, 55 (1989).
[38] M. J. Haun, E. Furman, S. J. Jang, and L. E. Cross, Ferroelectrics **99**, 63 (1989).
[39] T. Yamamoto and Y. Makino, Jpn. J. Appl. Phys. **35**, 3214 (1996).
[40] T. Yamamoto, Jpn. J. Appl. Phys. **37**, 6041 (1998).
[41] S. H. Oh and H. M. Jang, J. Appl. Phys. **85**, 2815 (1999).
[42] S. H. Oh and H. M. Jang, J. Am. Ceram. Soc. **82**, 233 (1999).
[43] S. H. Oh and H. M. Jang, Appl. Phys. Lett. **72**, 1457 (1998).
[44] A. Amin, M. J. Haun, B. Badger, H. A. McKinstry, and L. E. Cross, Ferroelectrics **65**, 107 (1985).
[45] T. R. Halemane, M. J. Haun, L. E. Cross, and R. E. Newnham, Ferroelectrics **62**, 149 (1985).
[46] T. R. Halemane, M. J. Haun, L. E. Cross, and R. E. Newnham, Ferroelectrics **70**, 153 (1986).
[47] C. L. Wang and S. R. P. Smith, J. Phys.: Condens. Matter **7**, 7163 (1995).
[48] V. M. Goldschmidt, Ber. Dtsch. Chem. Ges. B **60**, 1270 (1927).
[49] L. Pauling, J. Am. Chem. Soc. **69**, 542 (1947).
[50] R. D. K.-Smith and D. Vanderbilt, Phys. Rev. B **49**, 5828 (1994).
[51] A. M. Glazer and S. A. Mabud, Acta Crystallogr., Sect. B: Struct. Crystallogr. Cryst. Chem. **34**, 1060 (1978).
[52] S. Chattopadhyay, P. Ayyub, V. R. Palkar, and M. Multani, Phys. Rev. B **52**, 13 177 (1995).
[53] K. Ishikawa, K. Yoshikawa, and N. Okada, Phys. Rev. B **37**, 5852 (1988).
[54] W. L. Zhong, B. Jiang, P. L. Zhang, J. M. Ma, H. M. Chen, Z. H. Yang, and L. Li, J. Phys.: Condens. Matter **5**, 2619 (1993).
[55] H. Huang, Ph.D thesis, Nanyang Technological University, Singapore, 2000.
[56] N. Setter and R. Waser, Acta Mater. **48**, 151 (2000).